Ecotoxicology and Environmental Safety 166 (2018) 146–156

Contents lists available at ScienceDirect

Ecotoxicology and Environmental Safety

journal homepage: www.elsevier.com/locate/ecoenv

Six sources mainly contributing to the haze episodes and health risk assessment of $PM_{2.5}$ at Beijing suburb in winter 2016

Xianmang Xu[a], Hefeng Zhang[b], Jianmin Chen[a,c,d,*], Qing Li[c], Xinfeng Wang[a], Wenxing Wang[a], Qingzhu Zhang[a], Likun Xue[a], Aijun Ding[d], Abdelwahid Mellouki[a,c,e]

[a] School of Environmental Science and Engineering, Environment Research Institute, Shandong University, Ji'nan 250100, China
[b] Atmospheric Environment Institute, Chinese Research Academy of Environmental Sciences, Ministry of Environmental Protection (MEP), Beijing 100012, China
[c] Shanghai Key Laboratory of Atmospheric Particle Pollution and Prevention (LAP3), Fudan Tyndall Centre, Department of Environmental Science & Engineering, Fudan University, Shanghai 200433, China
[d] Institute for Climate and Global Change Research, School of Atmospheric Sciences, Nanjing University, Nanjing 210023, Jiangsu, China
[e] Institut de Combustion, Aérothermique, Réactivité et Environnement, CNRS, 45071 Orléans cedex 02, France

ARTICLE INFO

Keywords:
$PM_{2.5}$
Chemical characterization
PMF model
PSCF analysis
Health risk assessment

ABSTRACT

Aiming to a better understanding sources contributions and regional sources of fine particles, a total of 273 filter samples (159 of $PM_{2.5}$ and 114 of $PM_{1.0}$) were collected per 8 h during the winter 2016 at a southwest suburb of Beijing. Chemical compositions, including water soluble ions, organic carbon (OC), and elemental carbon (EC), as well as secondary organic carbon (SOC), were systematically analyzed and estimated. The total ions concentrations (TIC), OC, and SOC of $PM_{2.5}$ were with the following order: 16:00–24:00 > 08:00–16:00 > 00:00–08:00. Since primary OC and EC were mainly attributed to the residential combustion in the night time, their valley values were observed in the daytime (08:00–16:00). However, the highest ratio value of SOC/OC was observed in the daytime. It is because that SOC is easily formed under sunshine and relatively high temperature in the daytime. Positive matrix factorization (PMF), clustering, and potential source contribution function (PSCF) were employed for apportioning sources contributions and speculating potential sources spatial distributions. The average concentrations of each species and the source contributions to each species were calculated based on the data of species concentrations with an 8 h period simulated by PMF model. Six likely sources, including secondary inorganic aerosols, coal combustion, industrial and traffic emissions, road dust, soil and construction dust, and biomass burning, were contributed to $PM_{2.5}$ accounting for 29%, 21%, 17%, 16%, 9%, 8%, respectively. The results of cluster analysis indicated that most of air masses were transported from West and Northwest directions to the sampling location during the observation campaign. Several seriously polluted areas that might affect the air quality of Beijing by long-range transport were identified. Most of air masses were transported from Western and Northwestern China. According to the results of PSCF analysis, Western Shandong, Southern Hebei, Northern Henan, Western Inner Mongolia, Northern Shaanxi, and the whole Shanxi provinces should be the key areas of air pollution control in China. The exposure-response function was used to estimate the health impact associated with $PM_{2.5}$ pollution. The population affected by $PM_{2.5}$ during haze episodes reached 0.31 million, the premature death cases associated with $PM_{2.5}$ reached 2032. These results provided important implication for making environmental policies to improve air quality in China.

1. Introduction

In the past decades, the quantity of motor vehicles and energy consumption have an escalating increase by reasons of the rapid development of economy and industrialism and urbanization in China (Zhang et al., 2013). Meanwhile, air pollution is becoming increasingly severe with the progress and development of the human society. Pollution of fine particulate matter ($PM_{2.5}$) is one of the serious air pollution problems in northern China, especially in winter. $PM_{2.5}$ has been recognized as the key air pollutant of reducing visibility and harming human health (Tao et al., 2014; Chen et al., 2015; Fu and Chen, 2017). Several recent studies have indicated that many adverse health outcomes such as respiratory and cardiovascular morbidity and mortality are related with long-term exposure to highly PM (Hoek et al.,

* Corresponding author at: School of Environmental Science and Engineering, Environment Research Institute, Shandong University, Ji'nan 250100, China.
E-mail address: jmchen@fudan.edu.cn (J. Chen).

https://doi.org/10.1016/j.ecoenv.2018.09.069
Received 1 August 2018; Received in revised form 10 September 2018; Accepted 15 September 2018
Available online 25 September 2018
0147-6513/

2013; Weichenthal et al., 2014). The outdoor PM has been classified as one of carcinogens by the International Agency for Research on Cancer (IARC) which is a specialized cancer agency of the World Health Organization (WHO). $PM_{2.5}$ usually have a long atmospheric lifetime of days, which is beneficial to long-range transport in atmosphere and to deposition toward remote areas. During the long-range transport, $PM_{2.5}$ carries abundant anthropogenic pollutants and affects the global ecosystems (Mahowald, 2011). Those adverse health and environment problems are attributed to the harmful components in $PM_{2.5}$, including water soluble ions, OC, EC, and trace elements etc. (Zhang et al., 2013; Shi et al., 2014; Li et al., 2015).

To identify the source contributions to $PM_{2.5}$, the technique of source apportionment has been widely used around the world and also increasingly applied for the past decade in China (Hueglin et al., 2005; Chen et al., 2010; Tao et al., 2012; Zhang et al., 2013; Cao et al., 2011a, 2011b). Through statistical interpretation of ambient measurement, the contribution levels of different sources are quantitatively estimated by using receptor models. Generally, scholars identified the possible sources of $PM_{2.5}$ to be traffic and industrial emissions, dust storms, coal combustion, secondary inorganic aerosols, and biomass burning (He et al., 2001; Song et al., 2006; Tao et al., 2014; Chen et al., 2017). Secondary inorganic aerosols were divided into secondary sulfate, secondary nitrate, and secondary ammonium by using the chemical mass balance receptor model (CMB) (Zheng et al., 2005). Unfortunately, the source profiles must be provided when the source apportionment is concluded with CMB model. The measurements of source profiles are time-consuming and difficult work. A convenient and efficient analysis method is provided by positive matrix factorization (PMF) model. The PMF model developed by the Environmental Protection Agency (EPA) of USA is an easy and powerful tool in using factor analysis to identify the possible source contributions without the source profiles. Many cities such as Pittsburg (Zhou et al., 2004), Hong Kong (Lee et al., 1999), Chengdu (Tao et al., 2014), and Beijing (Wang et al., 2008; Song et al., 2006) have successfully applied the PMF model to identify the major sources and apportion source contributions. For example, Tao et al. (2014) identified six major sources including secondary inorganic aerosols, coal combustion, biomass burning, iron and steel manufacturing, Mo-related industries, and soil dust, and accounting for 37 ± 18, 20 ± 12, 11 ± 10, 11 ± 9, 11 ± 9, and 10 ± 12%, respectively, to $PM_{2.5}$ in Chengdu (an inland city in southwest China). This model provides a feasible alternative for the place lacked the local source profiles.

Several recent studies have attempted to identify the major sources of $PM_{2.5}$ based on the daily chemical compositions of $PM_{2.5}$ in different seasons in Beijing (Song et al., 2006; Yu et al., 2013; Zhang et al., 2013). Some sources and their contribution rates to $PM_{2.5}$ were simulated by PMF model. However, most of their studies focused on the chemical characterization and sources of $PM_{2.5}$ from seasonal perspective. In fact, the effect of human activities on the chemical compositions of $PM_{2.5}$ at different time periods of the day exhibits large diurnal variability. Better understanding of chemical characterization and source apportionment of $PM_{2.5}$ in haze episodes based on the diurnal variation will be high importance for air pollution control and human health protection.

In addition to source apportionment, the regional distribution of emission sources was also concerned by scholars. The potential source contribution function (PSCF) analysis has been successfully applied to identify potential regional sources (Polissar et al., 2001; Zhang et al., 2013; Li et al., 2015). The PSCF was computed by considering the backward trajectories and measured atmospheric pollutant concentrations using a geographical information system-based software, TrajStat (Wang et al., 2009). It is a conditional probability that air masses are probably responsible for pollutant concentrations higher than the criterion level when air masses arrive at the receptor site (Li et al., 2015). The operation of PSCF analysis was expound in Section 2.4.3.

Moreover, the health risk assessment associated with $PM_{2.5}$ is also one of the hot topics in air pollution studies. Generally, $PM_{2.5}$ has a higher adverse effect on human body than coarse particles (PM_{10}), which is because $PM_{2.5}$ can pass to the breathing system into human tissue and has systemic effects (Yin et al., 2017; Li et al., 2017; Miri et al., 2016, 2017). Epidemiological studies show $PM_{2.5}$ exposure can increase the risks of mortality and morbidity related to respiratory and cardiopulmonary diseases (Hammitt and Zhou, 2006; Xie et al., 2009; Liu et al., 2010; Huang and Zhang, 2013). Toxicological studies also suggest that $PM_{2.5}$ exposure can cause platelet activation and inflammation in lungs regions, which is closely related to increased risks of cardiovascular diseases and lung cancer (Frampton et al., 2012; Lippmann, 2014; Van Winkle et al., 2015; Miri et al., 2018). Heavy elements and polycyclic aromatic hydrocarbons (PAHs) in particles can also cause health risks to human body (Wang et al., 2018; Xu et al., 2016). Therefore, scholars hoped to estimate the health risk and help governments make environmental policies (Kan and Chen, 2004; Zhang et al., 2007; Li et al., 2013; Yin et al., 2015; Du and Li, 2016). Beijing as one of the polluted mega-cities in China, it is of great importance to evaluate and analyze the risk and cost of the health effects associated with $PM_{2.5}$ pollution in Beijing.

In this study, we continuously collected daily $PM_{2.5}$ and $PM_{1.0}$ samples with an eight-hour cycle during the winter in 2016 at a suburb site in Beijing. A suite of chemical species in particles including the major water soluble ions, OC, and EC were measured and analyzed. Furthermore, the major sources and source contributions of $PM_{2.5}$ were identified by using the PMF model. The potential source regions of chemical species in $PM_{2.5}$ were identified by employing the potential source contribution function analysis. Furthermore, the health exposure-response function was used to estimate the health risk due to $PM_{2.5}$ pollution. This study will provide significant information in making environmental policies and air management framework to reduce the current pollution level of $PM_{2.5}$ and improve the air quality in China.

2. Methodology

2.1. Site description

Beijing is the capital of China and located on the northern edge of the North China Plain. The total population of Beijing was 21.73 million in 2016 (Beijing Statistics Yearbook). The total motor vehicles increased to 5.72 million in 2016 compared to 5.20 million in 2012, and energy consumption was equivalent to 69.62 million tons of standard coal (Beijing Statistics Yearbook). The annual average concentration of $PM_{2.5}$ was 73 $\mu g\,m^{-3}$ in Beijing in 2016 and still fell short the national standard (35 $\mu g\,m^{-3}$), although all levels of government had made great efforts to reduce the levels of $PM_{2.5}$. The sampling station was located at southwest of Beijing (116°07′ E, 39°43′ N). The $PM_{2.5}$ transported from the southern of Hebei province where is regarded as one of the most polluted regions in China, would be collected when air masses pass through this sampling location. The samples were collected on the roof (21 m above ground) of an office building. There are few high-rise buildings within 100 m around the sampling station and no main pollution sources exist nearby. Thus, this observation could be considered as typical of the long-range transport pollution in Beijing.

2.2. Sample collection

Daily $PM_{2.5}$ and $PM_{1.0}$ samples were collected using two high volume air samplers (TH-1000F; Wuhan Tianhong Instruments Co. Ltd., China). The flow rate of samplers was calibrated before the start of the sampling campaign. The fine particles were collected on quartz fibre filters (Pallflex 2500 QAT-UP 8 × 10 in.) at a flow rate of 1.05 $m^3\,min^{-1}$. The quartz filters were baked at 500 °C for 3 h prior to sampling to remove carbonaceous impurities. The collected samples were stored

in the dark and at −20 °C in a freezer before chemical analysis to reduce evaporation of volatile components. The samples were collected with an eight-hour cycle (00:00–08:00; 08:00–16:00; 16:00–24:00 local time, LT) during 15 December 2016–4March 2017. A total of 273 samples (159 of $PM_{2.5}$ and 114 of $PM_{1.0}$) were collected and analyzed for water soluble ions, OC, and EC. Among the samples, 62 $PM_{2.5}$ filter samples were identified as heavy haze samples ($PM_{2.5} > 75\,\mu g\,m^{-3}$ and continue for days) and systematically analyzed. A field blank was collected with each sampler every ten days and then analyzed together with the samples.

2.3. Chemical analysis

2.3.1. Water soluble ions

A 47 mm diameter filter sample was cut from each filter and cut into pieces. Then samples and blank filters pieces were extracted with 25 mL ultrapurewater (specific resistivity = 18.2 MΩ cm; Millipore, Massachusetts, United States) using ultra-sonication for 1 h. At last, all extracted solution samples were filtered through a syringe with 0.2 μm filter (Xiboshi syringe filter, Tianjin Fuji Science and Technology Co., Ltd., China). Ionic species were analyzed with an ion chromatograph (Dionex ICS-90 and ICS-1500) equipped with a conductivity detector (ASRS-ULTRA). Anion species (F^-, Cl^-, NO_3^-, and SO_4^{2-}) were analyzed with a Dionex AS11-HC separator column. Cation species (Na^+, NH_4^+, K^+, Mg^{2+}, and Ca^{2+}) were analyzed with a CS12A separator column. The method detection limits (MDL) generally were 0.03–0.07 $\mu g\,m^{-3}$ for anion species and 0.01–0.04 $\mu g\,m^{-3}$ for cation species (Hsu et al., 2007).

2.3.2. OC and EC measurements

An area of 0.5 cm^2 punched from each sample was analyzed using a multiwavelength carbon analyzer (DRI model 2015, Magee Scientific Inc., USA) with seven wavelengths of 405, 450, 532, 635, 780, 808, and 980 nm following the IMPROVE_A protocol. This instrument is an expanded and updated version based on DRI model 2001 carbon analyzer. The output results of tests on samples show that OC and EC concentrations are same with those from conventional carbon analyzer with wavelength 635 nm for pyrolysis adjustment. Following the IMPROVE_A protocol, OC_1, OC_2, OC_3, and OC_4 were acquired at 140, 280, 480, and 580 °C in helium (He) atmosphere, respectively. And then the gas switched to a mixture of 2% oxygen in He, EC_1, EC_2, and EC_3 were acquired at 580, 740, and 840 °C, respectively. The concentrations of OC and EC were calculated by following equations: $OC = OC_1 + OC_2 + OC_3 + OC_4 + OP$; $EC = EC_1 + EC_2 + EC_3 - OP$, where OP is the optical pyrolyzed OC (Chow et al., 2007).

2.4. Data analysis methods

2.4.1. PMF model

The PMF model (version 5.0, EPA) was used to identify the source contributions. In order to ensure the program can run and reduce the uncertainty of PMF output results, few data that below the detection limit (BDL) were replaced with values corresponding to one-half the MDL (Lee et al., 2003). Chemical components including F^-, Cl^-, NO_3^-, SO_4^{2-}, Na^+, NH_4^+, K^+, Mg^{2+}, Ca^{2+}, OC, and EC were used for the PMF model analysis. The PMF analysis is only used to speculate the likely sources because of the lack of trace elements. Despite all that, this analysis still is of some significance for likely sources apportionment, especially when combined with previous studies in Beijing. In order to determine the number of factors, five, six, seven and even eight source factors were tested in practice. The base model was run 100 times to determine the objective function Q values effective. Different F_{peak} values were tested to determine the best. Finally, six-factor model with F_{peak} = -0.5 was decided. More detailed information of PMF model can be found in the studies by Prendes et al. (1999), Song et al. (2006) and Zhang et al. (2013).

2.4.2. Air mass back trajectory cluster

Three-day back trajectories of air masses initiated every 8 h arriving at sampling site at the height of 100 m a.s.l. were calculated using the HYSPLIT-4 model developed by the National Oceanic and Atmospheric Administration Air Resources Laboratory (NOAA-ARL) with a 1 × 1 resolution. The meteorological database were acquired from the Global Data Assimilation System (GDAS) of National Center for Environmental Prediction. The starting times were set at 00:00, 08:00, and 16:00 UTC corresponding to 08:00, 16:00, and 24:00 LT, respectively. Four air-mass trajectory clusters were classified using GIS-based software TrajStat (Wang et al., 2009).

2.4.3. Potential source contribution function (PSCF) analysis

The potential source contribution function (PSCF) analysis developed by Hopke et al. (1995) was used to identify the likely regional sources. The PSCF model is based on the HYSPLIT model, TrajStat as the computation tool to calculate backward trajectories and the pollutant concentrations assigned to each trajectory. The operation of PSCF model is a conditional probability that air masses are probably responsible for pollutant concentrations higher than the criterion level when air masses arrive at the receptor site (Li et al., 2015). The PSCF value in the *ij*th grid cell is defined as:

$$\mathrm{PSCF}_{ij} = \frac{m_{ij}}{n_{ij}}$$

where n_{ij} is designated as the total number of trajectory endpoints that fall in the *ij*th cell and m_{ij} is the number of polluted trajectory endpoints in the same cell.

In this study, the average concentrations were set as the polluted critical value, except for $PM_{2.5}$, OC, and EC. $PM_{2.5}$ was set at 75 $\mu g\,m^{-3}$ because this value corresponded to the threshold of mild pollution level in Air Quality Index (AQI) in China. OC and EC were set at bottom quartile because only the OC and EC concentrations in $PM_{2.5}$ during haze episodes were analyzed. The geophysical domain was in the range of 70–130°E, 25–55°N and divided into 7200 grid cells with a 0.5 × 0.5 resolution. To better reflect the uncertainty in cells due to the effect of small values of n_{ij} (Polissar et al., 2001), the weight function W_{ij} was adopted:

$$\mathrm{W}ij = \begin{cases} 1.00 & nij > 3nAve \\ 0.70 & 3nAve \geq nij > 1.5nAve \\ 0.42 & 1.5nAve \geq nij > nAve \\ 0.17 & nAve \geq nij > 0 \end{cases}.$$

2.5. Health risk assessment

The exposure-response functions were widely used to estimate the human health effects associated with air pollution in many epidemiological studies (Kan and Chen, 2004; Liu et al., 2010; Zhang et al., 2007; Li et al., 2013). This method is a proportion risk assessment model based on the Poisson regression (Du and Li, 2016). In this model, mortality and morbidity outcomes are usually considered as the health endpoints. Compared with population health, the selected health effects are small probability events conformed to Poisson distribution. Thus, cases at a given concentration C can be calculated with the following equations:

$$E_i = E_0 \exp[\beta_i(C - C_0)]$$

$$\Delta E = P(E_i - E_0) = P\left\{1 - \frac{1}{\exp[\beta_i(C - C_0)]}\right\}E_i$$

where C is the outdoor $PM_{2.5}$ concentration level ($\mu g\,m^{-3}$) in Beijing, C_0 is the baseline $PM_{2.5}$ concentration (in this study, C_0 = 25 $\mu g\,m^{-3}$, the 24-h average concentration of the WHO Air Quality Guidelines), β_i is the exposure-response coefficients obtained from the epidemiological studies in China, E_0 refers to the baseline incidence of certain health

Table 1
Statistics (means ± S.D.) concentrations (μg m^{-3}) of $PM_{2.5}$ and $PM_{1.0}$ chemical components.

Species	Overall		00:00–08:00		08:00–16:00		16:00–24:00	
	$PM_{2.5}$	$PM_{1.0}$	$PM_{2.5}$	$PM_{1.0}$	$PM_{2.5}$	$PM_{1.0}$	$PM_{2.5}$	$PM_{1.0}$
F^-	0.2 ± 0.2	0.2 ± 0.1	0.2 ± 0.1	0.2 ± 0.1	0.2 ± 0.1	0.2 ± 0.1	0.3 ± 0.2	0.2 ± 0.1
Cl^-	6.3 ± 3.9	4.6 ± 2.7	5.6 ± 3.4	4.4 ± 2.5	6.3 ± 3.7	4.4 ± 2.4	7.1 ± 4.7	5.1 ± 2.8
SO_4^{2-}	12.3 ± 10.6	7.3 ± 5.6	11.7 ± 9.5	7.0 ± 5.3	10.9 ± 10.2	8.0 ± 5.6	14.7 ± 11.9	8.7 ± 6.3
NO_3^-	5.5 ± 5.3	2.7 ± 1.7	5.1 ± 5.3	2.6 ± 1.2	4.8 ± 4.5	3.0 ± 1.8	6.7 ± 6.0	3.3 ± 2.1
Na^+	2.0 ± 0.7	1.9 ± 0.6	2.1 ± 0.8	1.9 ± 0.4	1.9 ± 0.6	2.1 ± 0.5	2.1 ± 0.8	2.0 ± 0.5
NH_4^+	10.5 ± 10.2	5.1 ± 3.5	9.7 ± 9.9	5.2 ± 3.1	9.0 ± 8.9	5.3 ± 3.3	13.3 ± 11.6	6.2 ± 3.8
K^+	2.5 ± 2.5	1.6 ± 2.3	2.0 ± 1.5	1.3 ± 0.8	2.6 ± 3.4	1.3 ± 0.8	2.8 ± 1.9	1.6 ± 1.0
Mg^{2+}	0.4 ± 0.3	0.4 ± 0.2	0.4 ± 0.3	0.2 ± 0.1	0.4 ± 0.3	0.4 ± 0.2	0.4 ± 0.2	0.4 ± 0.1
Ca^{2+}	2.7 ± 1.7	2.5 ± 1.3	3.1 ± 2.0	1.8 ± 1.1	2.3 ± 1.3	2.9 ± 1.3	2.7 ± 1.6	2.6 ± 1.3
Σ Ions	42.4 ± 30.0	26.3 ± 14.2	38.4 ± 26.9	24.6 ± 11.4	40.0 ± 28.5	27.5 ± 13.4	50.0 ± 34.1	30.1 ± 15.9
OC[a]	47.3 ± 21.9	–	41.7 ± 17.0	–	46.8 ± 24.5	–	55.7 ± 22.9	–
EC[a]	20.2 ± 13.2	–	19.6 ± 15.2	–	17.7 ± 12.9	–	24.1 ± 11.0	–
SOC[a]	15.5 ± 7.9	–	12.8 ± 5.8	–	16.7 ± 8.4	–	17.1 ± 8.8	–
$PM_{2.5}$	129.5 ± 136.1	–	–	–	–	–	–	–

[a] It only includes the concentrations of OC, EC and SOC during haze episodes. PM2.5 is daily average value in Beijing during observation campaign.

endpoint *i* of the total population, E_i refers to the incidence of the health endpoint *i* at the given concentration C, P is the total population, ΔE refers to the number of cases of health endpoint *i* attributed to $PM_{2.5}$ pollution. The values of parameters used in estimating process were explained in Section 3.4 and listed in Table 2.

3. Results and discussion

3.1. General characteristics and chemical components

The statistical summary of the atmospheric concentrations of water soluble ions, OC, and EC in $PM_{2.5}$ and $PM_{1.0}$ during sampling campaign is shown in Table 1. The mean concentration of $PM_{2.5}$ reached 129.5 ± 136.1 μg m^{-3}, which was 3 times higher than the national ambient air quality standards (NAAQS, 35 μg m^{-3}) and 12 times higher than the air quality guideline (annual average 10 μg m^{-3}) published by WHO (Tao et al., 2014). As well, it was nearly 2 times higher compared with the annual average concentration of $PM_{2.5}$ (73 μg m^{-3}) in Beijing in 2016. For ionic concentrations of $PM_{2.5}$, the mean concentration of SO_4^{2-} (12.3 ± 10.6 μg m^{-3}) ranked the highest among the water soluble ions followed by NH_4^+ (10.5 ± 10.2 μg m^{-3}), Cl^- (6.3 ± 3.9 μg m^{-3}), NO_3^- (5.5 ± 5.3 μg m^{-3}), Ca^{2+} (2.7 ± 1.7 μg m^{-3}), K^+ (2.5 ± 2.5 ± 1.7 μg m^{-3}), Na^+ (2.0 ± 0.7 μg m^{-3}), Mg^{2+} (0.4 ± 0.3 μg m^{-3}), and F^- (0.2 ± 0.2 μg m^{-3}). Such levels of mean concentrations are comparable to the previous study in Beijing (Zhang et al., 2013). However, the species order of ions contributions is different with the result by Zhang et al. (2013). In their study, the mean concentrations of ions were with the following order SO_4^{2-} (8.5 ± 8.6 μg m^{-3}) > NO_3^- (7.3 ± 8.1 μg m^{-3}) > NH_4^+ (4.5 ± 5.7 μg m^{-3}) > Cl^- (3.52 ± 3.32 μg m^{-3}) > Ca^{2+} (1.5 ± 0.9 μg m^{-3}) > Na^+ (1.08 ± 0.80 μg m^{-3}) > K^+ (0.81 ± 0.77 μg m^{-3}) > Mg^{2+} (0.18 ± 0.09 μg m^{-3}) in winter in Beijing. Different sampling locations and energy structure adjustment might be responsible for the change of species contributions in $PM_{2.5}$.

For diurnal variation, the Σ Ions of $PM_{2.5}$ were with the following order 16:00–24:00 (50.0 ± 34.1 μg m^{-3}) > 08:00–16:00 (40.0 ± 28.5 μg m^{-3}) > 00:00–08:00 (38.4 ± 26.9 μg m^{-3}). The diurnal variation of Σ Ions in $PM_{1.0}$ was similar to that of $PM_{2.5}$ following the order of 16:00–24:00 (30.1 ± 15.9 μg m^{-3}) > 08:00–16:00 (27.5 ± 13.4 μg m^{-3}) > 00:00–08:00 (24.6 ± 11.4 μg m^{-3}). It might mean that the concentrations of air pollutants reached up to peak values at nightfall and dropped to trough at early morning. It could be easily explained by the accumulation of pollutants due to human activities in daytime and the deposition of particles in the nighttime. The average concentrations of Σ Ions in $PM_{2.5}$ and $PM_{1.0}$ reached 42.4 ± 30.0 μg m^{-3} and 26.3 ± 14.2 μg m^{-3}, respectively. Diurnal variation of OC was similar to that of Σ Ions in $PM_{2.5}$ following the order of 16:00–24:00 (55.7 ± 22.9 μg m^{-3}) > 08:00–16:00 (46.8 ± 24.5 μg m^{-3}) > 00:00–08:00 (41.7 ± 17.0 μg m^{-3}). However, the diurnal variation of EC was somewhat different from those of OC and the Σ Ions in $PM_{2.5}$. The valley value of EC presented at 08:00–16:00 (17.7 ± 12.9 μg m^{-3}) instead of 00:00–08:00 (19.6 ± 15.2 μg m^{-3}). Coal combustion used for heating in the nighttime in winter might be responsible for the high concentrations of EC in the nighttime. The average concentrations of OC and EC reached 47.3 ± 21.9 μg m^{-3} and 20.2 ± 13.2 μg m^{-3}, respectively. The concentrations of OC and EC were higher than those of OC (24.9 ± 15.6 μg m^{-3}) and EC (7.5 ± 7.4 μg m^{-3}) in winter by Zhang et al. (2013), which might be caused by only the OC and EC during haze episodes were analyzed.

3.1.1. Water soluble ions during haze episodes

Three air pollution events of haze episodes during sampling campaign were selected as typical cases and separately analyzed. The time series of concentrations of water soluble ions and total ions concentrations (TIC) are plotted in Fig. 1. SO_4^{2-}, NH_4^+, Cl^-, and NO_3^- were still the major species in $PM_{2.5}$ during haze episodes. However, the order of species contributions during haze episodes was different from that during the entire sampling campaign, with the following order SO_4^{2-} (22.8 ± 10.0 μg m^{-3}), NH_4^+ (20.7 ± 10.1 μg m^{-3}), NO_3^- (10.9 ± 5.4 μg m^{-3}), Cl^- (9.2 ± 3.6 μg m^{-3}), K^+ (3.9 ± 1.6 μg m^{-3}), Na^+ (2.4 ± 0.6 μg m^{-3}), Ca^{2+} (2.1 ± 1.5 μg m^{-3}), Mg^{2+} (0.4 ± 0.2 μg m^{-3}), and F^- (0.3 ± 0.1 μg m^{-3}). Nearly all of species were increased with different levels in the processes of air pollution episodes, except for the slightly decreased Ca^{2+} and Mg^{2+}. Ca^{2+} and Mg^{2+} might mainly come from dust and could be considered as markers of dust (Song et al., 2006) (explain later in Section 3.2). It does seem to imply that the mass of dust in atmosphere doesn't have much change whether haze or fine days. In addition, the relative contribution of dust in $PM_{2.5}$ might be more higher in non-haze days, which suggested a certain amount of dust were probably come from long-range transport.

Diurnal variation of TIC during haze events was illustrated in Fig. 1 and summarized in Fig. 1d. Most of peak values of TIC presented at 16:00–24:00, which was consistent with previous statistical results of overall samples. The mean values of TIC in different time periods of day were calculated following the order of 16:00–24:00 (84.0 ± 26.4 μg m^{-3}) > 08:00–16:00 (71.5 ± 23.7 μg m^{-3}) > 00:00–08:00 (65.0 ± 25.3 μg m^{-3}). The mean concentration of TIC reached 73.7 ± 25.9 μg m^{-3} in haze episodes, which was nearly 2 times higher compared with that of overall samples in this observation and nearly 3 times higher compared with the result by Zhang et al. (2013) in winter.

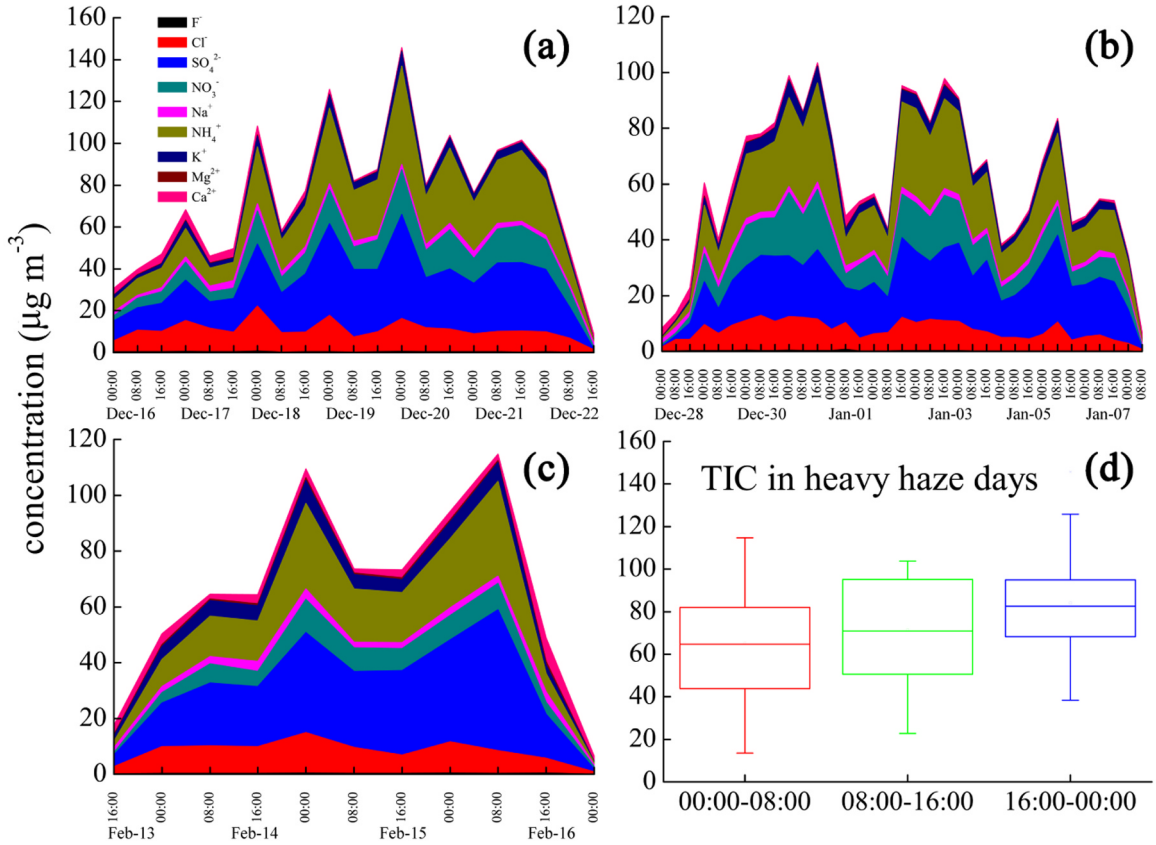

Fig. 1. Diurnal variation of water soluble ions during three haze events.

3.1.2. OC, EC and SOC during haze episodes

EC is usually considered as a primary pollutant, and OC is suggested from both primary sources and secondary sources transformed from gaseous precursors (Jimenez et al., 2009). The contributions of both OC_{pri} and SOC to carbonaceous during haze episodes were calculated using the EC tracer method with the following equations (Hou et al., 2011):

$$OCpri = EC \times (OC/EC)pri$$
$$SOC = OCtot - OCpri$$

where OC_{pri} is designated as the primary OC, $(OC/EC)_{pri}$ is the ratio of OC to EC in the primary aerosol, SOC is the secondary OC, and OC_{tot} is the total OC.

The ratio of OC to EC in the primary aerosol is usually difficult to estimate. Scholars suggested that the value of $(OC/EC)_{pri}$ could be replaced by the minimum ratio of OC/EC (Castro et al., 1999; Hou et al., 2011). The minimum ratio of OC/EC in $PM_{2.5}$ was calculated to be 1.7 within the confidence interval ($p = 0.05$), which was comparable to those results measured in other urban areas, such as 1.5 in Long Beach (Turpin and Huntzicker, 1995) and 1.6 in Shanghai (Hou et al., 2011). According to this result, the average concentrations of SOC in $PM_{2.5}$ during haze episodes were calculated and shown in Table 1. Diurnal variation of SOC was similar to those of TIC and OC in $PM_{2.5}$ in haze events following the order of 16:00–24:00 ($17.1 \pm 8.8\,\mu g\,m^{-3}$) > 08:00–16:00 ($16.7 \pm 8.4\,\mu g\,m^{-3}$) > 00:00–08:00 ($12.8 \pm 5.8\,\mu g\,m^{-3}$), accounting for 32.6 ± 12.3%, 40.5 ± 15.9%, and 32.4 ± 15.0% to OC, respectively. The highest contribution rate of SOC to OC presented in 08:00–16:00 period, which related to the formation conditions of SOC. For instance, the semi-volatile organic compounds with a lower molecular weight are mostly in gaseous phase and easily transformed to SOC due to sunshine and proper temperature in the daytime (Ye et al., 2017; Yassaa et al., 2001). The average concentration of SOC reached $15.5 \pm 7.9\,\mu g\,m^{-3}$, accounting for 34.9 ± 14.6% to OC during haze episodes.

The ratios of OC/EC can be used to preliminary estimate the sources of carbonaceous aerosols (Turpin and Huntzicker, 1995). However, the ratios of OC/EC usually have large discrepancies and variability in different sources. For example, the OC/EC ratios of biomass burning mostly fell within the range of 4.1–14.5, coal combustion within 0.3–7.6, and vehicle emission within 0.7–2.4 (Watson et al., 2001). In this work, the ratios of OC/EC mostly fell within the range of 1.0–4.8. The OC/EC ratios and linear regression equations in different time periods during haze episodes are shown in Fig. 2a. The mean OC/EC ratios were represented with the slopes of 1.7 ($R^2 = 0.86$), 2.4 ($R^2 = 0.94$), and 2.2 ($R^2 = 0.95$) in 00:00–08:00, 08:00–16:00, and 16:00–24:00, respectively. These mean ratios were similar to those results in winter in previous studies, such as 2.66 in Beijing (Zhang et al., 2013) and 2.6 in Chengdu (Tao et al., 2014). The formation of SOC should be responsible for the high ratio of OC/EC presented at 08:00–16:00. Moreover, OC and EC in Beijing were well correlated in each time period, which suggested that OC and EC were derived from similar sources during haze episodes.

3.1.3. Relative contributions of chemical components to $PM_{2.5}$ during haze episodes

The proportions of chemical components including water soluble ions, OC_{pri}, EC, and SOC in $PM_{2.5}$ were schematically illustrated by four pie charts for three time periods and overall samples during haze episodes (Fig. 2b). In summary, the contributions of water soluble ions to $PM_{2.5}$ were almost equal to those of carbonaceous aerosols. In terms of ions, the major components were SO_4^{2-}, NH_4^+, NO_3^-, and Cl^-, accounting for 7.95%, 7.51%, 3.73%, and 3.39% during haze episodes. For diurnal variation, the secondary inorganic aerosols including

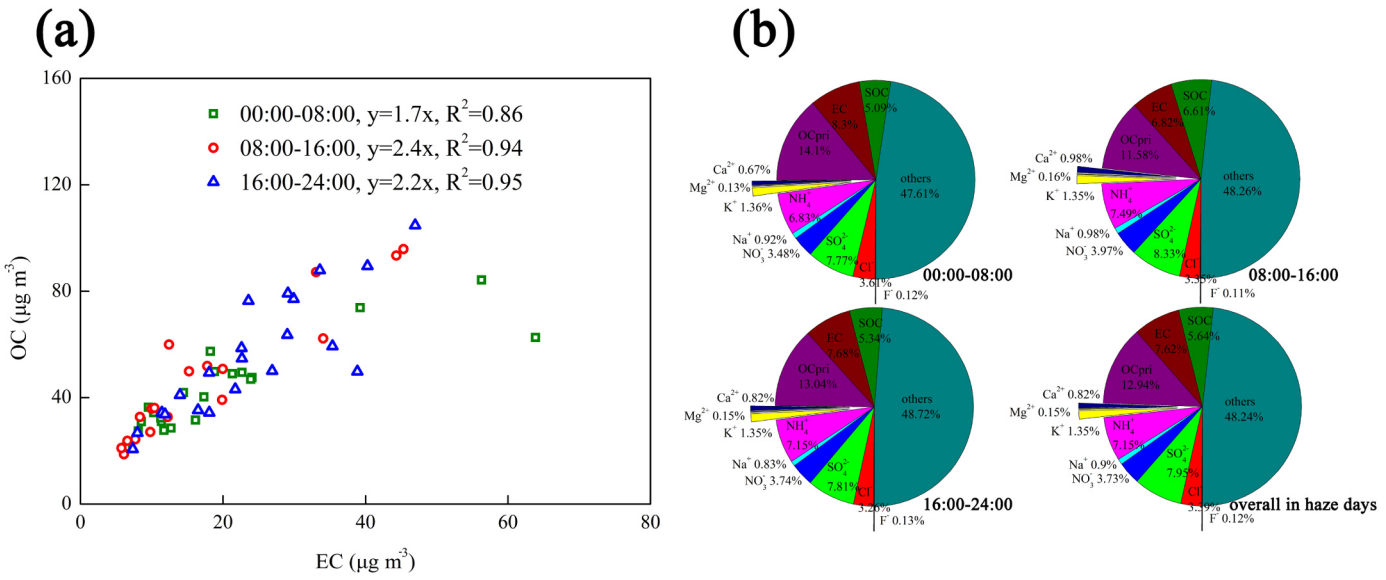

Fig. 2. Linear regression equations of OC vs. EC and chemical components contributions to $PM_{2.5}$.

sulfate, ammonium, and nitrate had the largest proportion at all time periods during haze episodes. The totals of secondary inorganic species (SO_4^{2-}, NH_4^+, and NO_3^-) were calculated, accounting for 18.08%, 19.79%, and 18.70% in 00:00–08:00, 08:00–16:00, and 16:00–24:00, respectively. Nevertheless, the proportion of Cl^- was higher than NO_3^- reached 3.61% in 00:00–08:00 period, which might be similar to EC related to the emission of Cl^- from coal combustion used for heating in the nighttime in northern China. For carbonaceous aerosols, OC_{pri}, EC, and SOC were calculated accounting for 12.94%, 7.62%, and 5.64%, respectively. The SOC peaks were observed in 08:00–16:00 accounting for 6.61% due to the advantage conditions and factors for the formation of SOC in daytime. Whereas the valley values of OC_{pri} and EC were also observed in 08:00–16:00 accounting for 11.58% and 6.82%, respectively, which suggested that the source contribution of coal combustion in the nighttime in winter played a dominant role for the concentrations of OC_{pri} and EC. This diurnal variational characteristic of OC_{pri} and EC indirectly verifies the reliability of the PMF results in the next section.

Other unidentified components including highly volatile components, trace elements, and other unmeasured species accounted for 48.24% in haze episodes. This proportion of unidentified components was comparable to the results by Zhang et al. (2013) in winter in Beijing. In their study, the crustal elements, such as Al, Si, Ca, Fe, Ti and Mg were included in mineral dust which was estimated, and accounting for 28.9% in $PM_{2.5}$ in winter. And the trace element oxide accounted for 0.4% in $PM_{2.5}$. Even so, they also had a lot of components were unidentified, which accounting for 22.0% in $PM_{2.5}$. They suggested that it could be attributed to water absorption of ions in the weighing environment, volatilization of some species, and the error of estimation method (Speer et al., 1997; Ying and Kuo, 2005; Zhang et al., 2013).

3.2. Source apportionment with PMF

The likely main sources were identified using the PMF model. Six factors including secondary inorganic aerosols, coal combustion, industrial and traffic emissions, road dust, soil and construction dust, and biomass burning, were considered as the major sources to $PM_{2.5}$, and accounting for 29%, 21%, 17%, 16%, 9%, and 8%, respectively. Modeled source profiles and the relative contributions of identified main sources to each analyzed species are shown in Fig. 3. The average concentrations of each species and the source contributions to each species were calculated based on the data of species concentrations with an 8 h period simulated by PMF model. The PMF model provides the feasibility for source apportionment of $PM_{2.5}$.

The first factor was considered as a mixed source of industrial and traffic emissions which provided 23 ± 12 μg m^{-3} aerosol mass in $PM_{2.5}$ derived by PMF model. This source almost involved all analyzed species, and with high contents of OC, SO_4^{2-}, NO_3^-, NH_4^+, and F^- (Yao et al., 2016). Besides chemical industry technique emissions, it also involved the emissions from energy fuel used in industrial processes and transportation. The emissions from waste incineration plants might also be included in this source due to a certain level of K^+ was simulated by PMF model. Coal and oil are the primary energy sources commonly used in industries and traffic in China. The emissions of energy and fuel combustion are the main sources of primary OC and F^- (Cao et al., 2011a, 2011b; Zhang et al., 2013; Xu et al., 2018). The contribution of industrial and traffic emissions was 17%, which was slightly higher than the 14% apportioned by Zhang et al. (2013). It might be related to the gradually increased number of motor vehicles and the difference of sampling locations in Beijing.

The second source is secondary inorganic aerosols, which is characterized by high contents of NH_4^+, NO_3^-, and SO_4^{2-} (Zhang et al., 2013; Yao et al., 2016). This source provided 42 ± 24 μg m^{-3} aerosol mass in $PM_{2.5}$. The secondary inorganic aerosols mainly includes secondary sulfates and secondary nitrate. Secondary sulfates were formed from the oxidation of SO_2 by photochemical reactions. Secondary nitrates were formed from the oxidation of NO_x. SO_2 and NO_x were mainly emitted from coal and oil combustion, which could be interacted with NH_3 under certain conditions. Therefore, it was reasonable that those three ions were considered as markers of secondary inorganic aerosols. The contribution of this source was 29%, which was slightly small than the 31% by Song et al. (2006) and equal to the result of CMB model by Zheng et al. (2005).

The third factor was considered as road dust, which was identified by high Ca^{2+}, Mg^{2+}, OC, and EC. This source provided 22 ± 16 μg m^{-3} aerosol mass in $PM_{2.5}$. Compared with soil dust, road dust is more exposed to human activities (Song et al., 2006). The high values of OC, EC, SO_4^{2-}, NH_4^+ and NO_3^- could be attributed to rotted vegetation and rubbish, traffic emissions, and coal combustion in urban. Although the fourth source of soil and construction dust also has a high value of Ca^{2+} and Mg^{2+}, the values of SO_4^{2-}, NH_4^+ and NO_3^- in soil dust are lower than those of road dust. The source of soil and construction dust provided 13 ± 13 μg m^{-3} aerosol mass in $PM_{2.5}$. The

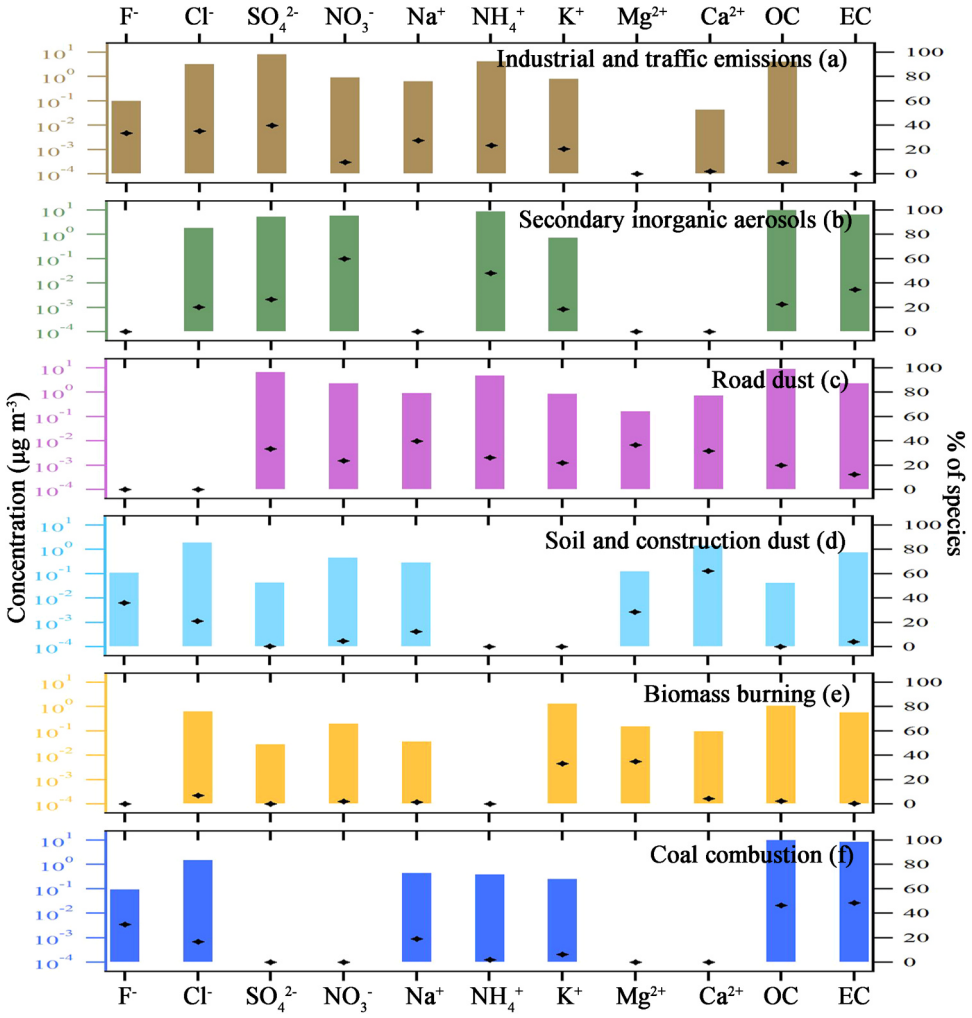

Fig. 3. Six source profiles (bars) identified from the PMF model and contribution percentages (black dots) from each source.

sum contribution (25%) of road dust (16%) and soil and construction dust (9%) was higher than 16% by Zhang et al. (2013) and the 20% by Zheng et al. (2005), which was probably related to the sampling site located at suburb in Beijing. More soil dust could be transported to observation site from near or far regions because there was no obstruction from tall buildings.

The fifth source is biomass burning, which is characterized by high K^+, OC, and EC (Zhang et al., 2013; Li et al., 2016). Generally, this factor has higher contributions in spring and autumn than summer and winter. In this study, it provided 12 ± 18 μg m^{-3}aerosol mass, and accounting for 8% of $PM_{2.5}$, which was very close to the 7% in winter in Beijing by Zhang et al. (2013).

The last factor was considered as coal combustion, which was characterized by high OC, EC, Cl^- and F^- (Zhang et al., 2013; Zong et al., 2016). The high Cl^- associated with particles aerosols in winter is a distinctive feature in northern China due to the emissions from coal combustion (Wang et al., 2008; Zhang et al., 2013). Coal combustion is suggested as a primary source of $PM_{2.5}$ in China (Yao et al., 2009), which has led to serious air pollution problem in China and even a larger regional scale. In this study, the source of coal combustion provided 29 ± 18 μg m^{-3} aerosol mass, and accounting for 21% to $PM_{2.5}$. It was slightly higher than the 19% by Song et al. (2006) and much lower than the 57% by Zhang et al. (2013). The factor of secondary inorganic aerosols, the precursors SO_2 and NO_x were mainly emitted from the fuel combustion including coal and oil, while this factor was not considered in the study by Zhang et al., which might be the main cause of the large difference.

3.3. Transport and regional sources

3.3.1. Trajectory cluster of long-range transport

The 72 h back trajectories starting at the height of 100 m at sampling site were calculated using HYSPLIT-4 model with an 8 h period. The back trajectories were classified into four clusters using TrajStat in this work (Fig. 4). Back trajectories were mainly in a 90° range between North (N) and West (W). The trajectory clusters were dominated by both West and West by North, accounting for 46.03% and 31.75%, respectively. The other two trajectory clusters were North and North by West directions, accounting for 9.52% and 12.70%, respectively. The results of cluster analysis indicated that most of air masses were transported from West and Northwest directions to the sampling location during the observation campaign. The long-range transport of air pollutants have a profound effect on local air quality in Beijing (Wang et al., 2004). Furthermore, the spatial distribution of regional sources would be identified with the PSCF analysis in the next section.

3.3.2. Potential source region distributions with PSCF

The likely regional sources were identified with PSCF analysis and illustrated in Fig. 5. In this work, the contributions of regional sources associated with $PM_{2.5}$ and its species were estimated using a weight function. The PSCF results showed that the fine particles transported to Beijing was primarily originated from northwestern China in winter. The highest PSCF values of F^- mainly presented in northern China including the Loess Plateau, Western Inner Mongolia, Northern Ningxia, Northern Shaanxi, and Shanxi province, which could be suggested that

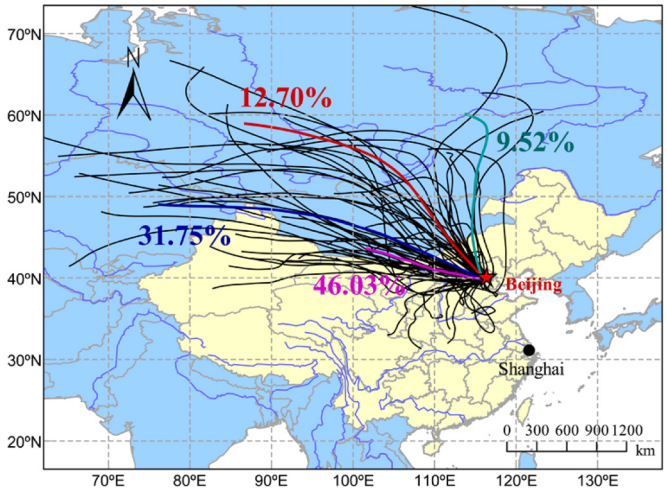

Fig. 4. Clustering analysis of 72 h back trajectories starting at height of 100 m at sampling site during the sampling periods.

F^- might mainly come from the particles transported from these areas besides energy combustion (Fig. 5a). Cl^- and Na^+ exhibited similar source region distributions (Fig. 5b and e). The Loess Plateau, Western Inner Mongolia, and Outer Mongolia were important source regions and pathways for Cl^- and Na^+. Moreover, Northern Henan, Southern Hebei, and Western Shandong were also very important source regions for Cl^- and Na^+. SO_4^{2-}, NO_3^-, and NH_4^+ were more likely come from similar source regions (Fig. 5c, d, and f), which were identified primarily from Western Shandong, Northern Henan, Southern Hebei, and the southeast of Shanxi. Many industries are located in these areas, which may be an important factor for pollutants emissions. The source regions of K^+ mainly included Western Shandong, Southern Hebei, and a small area in Northern Henan (Fig. 5g). Shandong, Henan, and Hebei provinces are the major agricultural regions in China. In general, K^+ can be considered as an important symbol of biomass burning. Therefore, K^+ might be likely come from straw burning in those areas. As shown in Fig. 5h and i, the ions of Mg^{2+} and Ca^{2+} might be attributed to the long-range transport of mineral dusts from Western Inner Mongolia and Outer Mongolia. OC and EC as important markers of coal combustion exhibited similar source region distributions with those of SO_4^{2-}, NO_3^-, and NH_4^+ (Fig. 5j and k). Coal as an import energy fuel were used in large quantities in those industrial area, which should be an important reason for the highest PSCF values of OC and EC appeared at those areas. At last, the result of the PSCF analysis for $PM_{2.5}$ is shown in Fig. 5l. The potential source regions of $PM_{2.5}$ mainly included Western Shandong, Southern Hebei, Western Inner Mongolia, Northern Shaanxi, and the whole Shanxi province.

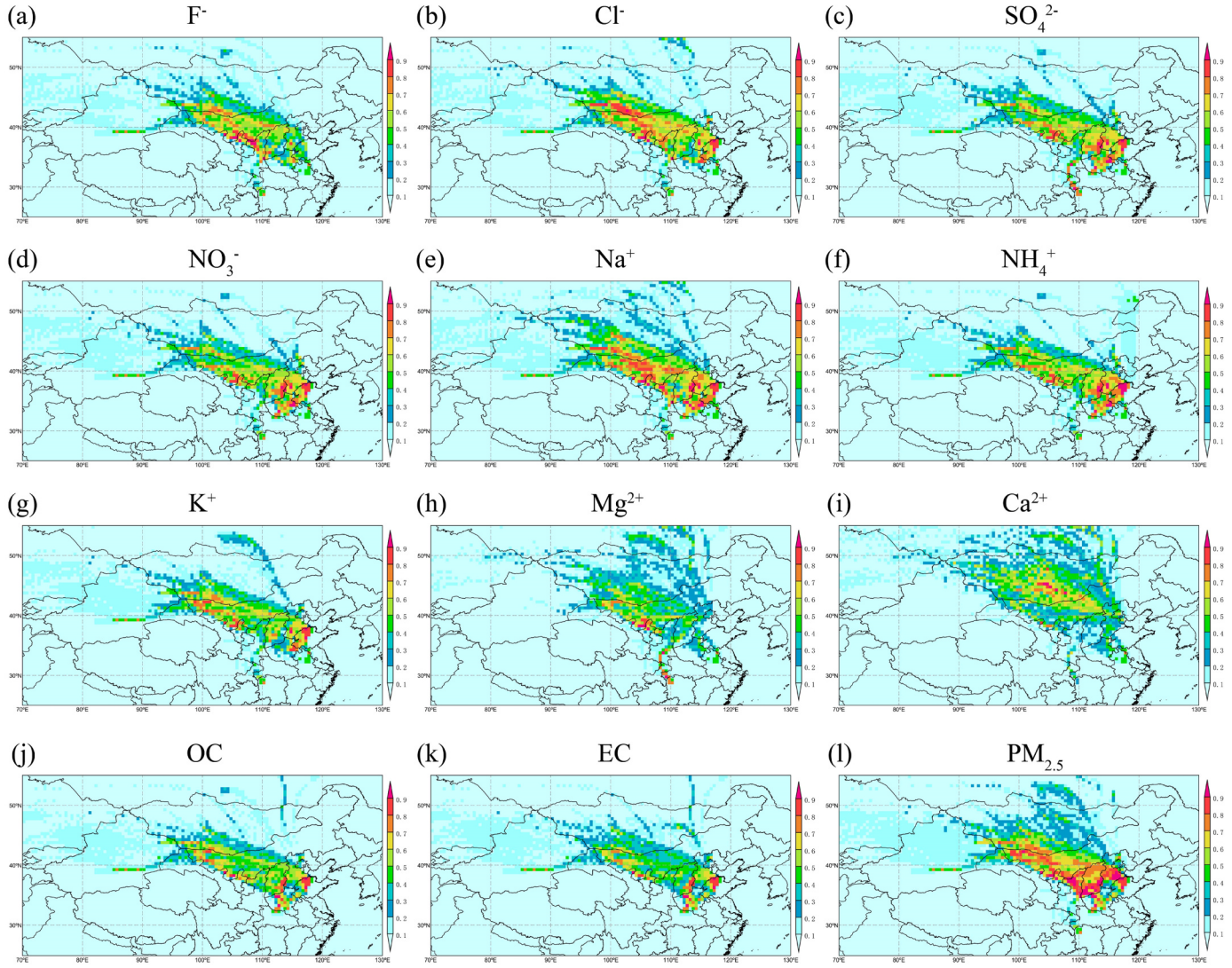

Fig. 5. The potential source contribution function (PSCF) analysis.

Table 2
Health risk assessment of $PM_{2.5}$ during haze episodes in Beijing ($C_0 = 25\,\mu g\,m^{-3}$).

Health endpoints	Coefficients β_i (95% CI)	Incidence	Event 1	Event 2	Event 3	Sum	Annual %[a]
All-cause mortality	0.0090 (0, 0.0180) (Cao et al., 2011a)	0.00662 (PHPHRB, 2016)	690	1180	161	2032	1.4
Respiratory mortality	0.0143 (0.0085, 0.0201) (Xie et al., 2009)	0.00065 (PHPHRB, 2016)	117	203	27	347	2.5
Cardiovascular mortality	0.0053 (0.0015, 0.0090) (Xie et al., 2009)	0.00170 (PHPHRB, 2016)	98	167	23	289	0.8
Lung-cancer mortality	0.0340 (0, 0.0710) (Cao et al., 2011a)	0.00064 (PHPHRB, 2016)	389	712	80	1181	8.5
Respiratory hospital admission	0.0109 (0, 0.0221) (Xie et al., 2009)	0.01203 (ICBMHFBC, 2016)	1567	2690	363	4620	1.8
Cardiovascular hospital admission	0.0068 (0.0043, 0.0093) (Xie et al., 2009)	0.02431 (ICBMHFBC, 2016)	1850	3148	436	5433	1.0
Outpatient visits internal medicine (0–14 years old)	0.0056 (0.0020, 0.0090) (Liu et al., 2010)	0.15300 (Liu et al., 2010)	9406	15,970	2230	27,606	0.8
Outpatient visits Pediatrics (> 14 years old)	0.0049 (0.0027, 0.0070) (Liu et al., 2010)	0.41105 (Liu et al., 2010)	21,870	37,079	5200	64,150	0.7
Acute bronchitis	0.0566 (0.0444, 0.0688) (Yin et al., 2015)	0.03800 (Huang and Zhang, 2013)	60,311	120,179	10,558	191,048	23.1
Chronic bronchitis	0.0195 (0.0155, 0.0235) (Yin et al., 2015)	0.00694 (Huang and Zhang, 2013)	3740	6555	829	11,124	7.4
Asthma attack	0.0210 (0.0145, 0.0274) (Huang and Zhang, 2013)	0.00940 (Huang and Zhang, 2013)	2795	4918	615	8328	4.1
Sum			102,230	191,719	20,393	314,342	

[a] Total cases of each health endpoint/annual cases of this health endpoint.

3.4. Health effects of $PM_{2.5}$ during haze episodes

Table 2 shows the health exposure-response coefficients and baseline incidence rates used for health risk assessment in this study. To increase its regional accuracy of exposure-response coefficients, the studies performed in China were given priority. The baseline incidence rates were obtained from the Public Health and Population Health Report of Beijing (PHPHRB, 2016), the Information Center of Beijing Municipal Health and Family Planning Commission (ICBMHFBC, 2016), and some studies performed in China. Three specific-cause mortalities including respiratory, cardiovascular and lung-cancer were estimated to identify which was the major cause to the all-cause mortality. Moreover, other health endpoints including respiratory and cardiovascular hospital admission, internal medicine and pediatrics outpatient visits, acute and chronic bronchitis, and asthma attack were also estimated in this work.

Table 2 also reports the health effects calculated with the baseline concentration $C_0 = 25\,\mu g\,m^{-3}$ in Beijing during the major three haze events in winter 2016. The population affected by $PM_{2.5}$ during these three haze events reached 0.31 million, accounting for 1.4% to the total population (21.73 million) of Beijing. The number of cases of acute bronchitis was higher compared with other health endpoints, accounting for 23.1% of the total number of annual cases of this disease in 2016. In terms of mortality, the summation of all-cause mortality associated with $PM_{2.5}$ was 2032, accounting for 1.4% of annual death toll in Beijing in 2016. The cases of premature deaths due to $PM_{2.5}$ were lower than those for long-term exposure studies in China, which because of only the health risks during haze episodes were estimated in this study (Yin et al., 2015, 2017). However, it was comparable to those for short-term exposure studies in China (Xie et al., 2014; Du and Li, 2016). Among the excess deaths due to $PM_{2.5}$, the cases of premature deaths due to respiratory disease, cardiovascular disease and lung cancer were 347, 289 and 1181, accounting for 2.5%, 0.8% and 8.5% respectively to the annual cases of these health endpoints. The lung cancer contributed the highest number of premature deaths due to $PM_{2.5}$. According to the report by the PHPHRB, cancer was the number one cause of disease deaths in Beijing in 2016, and accounting for 26.8% to all disease deaths. Furthermore, lung cancer was the leading cause among all kinds of malignant cancers, accounting for 31.4% to all deaths due to cancer. In this study, the lung cancer due to $PM_{2.5}$ was accounting for 58.1% to premature deaths associated with $PM_{2.5}$. Therefore, $PM_{2.5}$ pollution should be one of the reasons for the increasing of cancer mortality year by year in Beijing.

4. Conclusions

The mean concentration of $PM_{2.5}$ reached $129.5 \pm 136.1\,\mu g\,m^{-3}$ in the whole observation campaign in Beijing, which is 3 times greater than the NAAQS standard ($35\,\mu g\,m^{-3}$). An interesting diurnal variation was observed, which indicated the total ions concentrations of $PM_{2.5}$ were with the following order: 16:00–24:00 > 08:00–16:00 > 00:00–08:00. However, the valley values of OC_{pri} and EC were observed in 08:00–16:00 instead of 00:00–08:00, which was attributed to the coal combustion used in the nighttime for heating in winter in northern China. SOC was estimated and following the same order with total ions concentrations. But the highest ratio value of SOC/OC was in 08:00–16:00 due to that SOC was easily formed under sunshine and proper temperature condition in the daytime. Furthermore, Six likely sources were identified using the PMF model. Modeled source profiles and their relative contributions to each analyzed species were analyzed. Secondary inorganic aerosols and coal combustion were the dominant sources of $PM_{2.5}$, accounting for half of all factors contributions. According to back trajectories at sampling location, four trajectory clusters were estimated and expound. The $PM_{2.5}$ from long-range transport were mainly from the northwest China. According to the results of PSCF analysis, Western Shandong, Southern Hebei, Northern Henan, Western Inner Mongolia, Northern Shaanxi, and the whole Shanxi provinces should be the key areas of air pollution control in China to improve air quality in Beijing. At last, the health risk associated with $PM_{2.5}$ pollution was estimated with the health exposure-response functions in this study. The cases of premature deaths due to $PM_{2.5}$ during haze episodes reached 2032, accounting for 1.4% of annual death toll in Beijing in 2016.

Acknowledgments

This work was supported by the Ministry of Science and Technology of China (No. 2016YFC0202700), the National Natural Science Foundation of China (No. 91743202, 21527814) and Marie Skłodowska-Curie Actions, EU (690958-MARSU-RISE-2015).

Conflict of interest

The authors declare that they have no competing financial interests.

References

Cao, J., Yang, C., Li, J., Chen, R., Chen, B., Gu, D., Kan, H., 2011a. Association between long-term exposure to outdoor air pollution and mortality in China: a cohort study. J.

Hazard. Mater. 186 (2–3), 1594–1600.
Cao, J., Chow, J.C., Tao, J., Lee, S., Watson, J.G., Ho, K.F., Wang, G., Zhu, C., Han, Y., 2011b. Stable carbon isotopes in aerosols from Chinese cities: influence of fossil fuels. Atmos. Environ. 45 (6), 1359–1363.
Castro, L.M., Pio, C., Harrison, R.M., Smith, D., 1999. Carbonaceous aerosol in urban and rural European atmospheres: estimation of secondary organic carbon concentrations. Atmos. Environ. 33 (17), 2771–2781.
Chen, H., Hu, D., Wang, L., Mellouki, A., Chen, J., 2015. Modification in light absorption cross section of laboratory-generated black carbon-brown carbon particles upon surface reaction and hydration. Atmos. Environ. 116, 253–261.
Chen, J., Li, C., Ristovski, Z., Milic, A., Gu, Y., Islam, M.S., Wang, S., Hao, J., Zhang, H., He, C., Guo, H., Fu, H., Miljevic, B., Morawska, L., Thai, P.K., Lam, Y.F., Pereira, G., Ding, A., Huang, X., Dumka, U.C., 2017. A review of biomass burning: emissions and impacts on air quality, health and climate in China. Sci. Total Environ. 579, 1000–1034.
Chen, L.W., Lowenthal, D.H., Watson, J.G., Koracin, D., Kumar, N., Knipping, E.M., Wheeler, N.J.M., Craig, K.J., Reid, S.B., 2010. Toward effective source apportionment using positive matrix factorization: experiments with simulated PM2.5 data. J. Air Waste Manag. Assoc. 60 (1), 43–54.
Chow, J.C., Watson, J.G., Chen, L.W., Chang, M.C.O., Robinson, N.F., Trimble, D., Kohl, S.D., 2007. The IMPROVE_A temperature protocol for thermal/optical carbon analysis: maintaining consistency with a long-term database. J. Air Waste Manag. Assoc. 57 (9), 1014–1023.
Du, Y., Li, T., 2016. Assessment of health-based economic costs linked to fine particulate ($PM_{2.5}$) pollution: a case study of haze during January 2013 in Beijing, China. Air Qual. Atmos. Health 9 (4), 439–445.
Frampton, M.W., Bausch, J., Chalupa, D.C., Hopke, P.K., Little, E.L., Oakes, D., Stewart, J.C., Utell, M.J., 2012. Effects of outdoor air pollutants on platelet activation in people with type 2 diabetes. Inhal. Toxicol. 24 (12), 831–838.
Fu, H., Chen, J., 2017. Formation, features and controlling strategies of severe haze-fog pollutions in China. Sci. Total Environ. 578, 121–138.
Hammitt, J.K., Zhou, Y., 2006. The Economic Value of Air-Pollution-Related Health Risks in China: A Contingent Valuation Study. Environ. Resour. Econ. 33 (3), 399–423.
He, K., Yang, F., Ma, Y., Zhang, Q., Yao, X., Chan, C.K., Cadle, S.H., Chan, T., Mulawa, P.A., 2001. The characteristics of PM2.5 in Beijing, China. Atmos. Environ. 35 (29), 4959–4970.
Hoek, G., Krishnan, R.M., Beelen, R., Peters, A., Ostro, B., Brunekreef, B., Kaufman, J.D., 2013. Long-term air pollution exposure and cardio-respiratory mortality: a review. Environ. Health 12 (1), 43.
Hopke, P.K., Barrie, L.A., Li, S., Cheng, M., Li, C., Xie, Y., 1995. Possible sources and preferred pathways for biogenic and non-sea-salt sulfur for the high Arctic. J. Geophys. Res. Atmos. 100 (D8), 16595–16603.
Hou, B., Zhuang, G., Zhang, R., Liu, T., Guo, Z., Chen, Y., 2011. The implication of carbonaceous aerosol to the formation of haze: revealed from the characteristics and sources of OC/EC over a mega-city in China. J. Hazard. Mater. 190 (1–3), 529–536.
Hsu, S., Liu, S.C., Kao, S., Jeng, W., Huang, Y., Tseng, C., Tsai, F., Tu, J., Yang, Y., 2007. Water-soluble species in the marine aerosol from the northern South China Sea: high chloride depletion related to air pollution. J. Geophys. Res. Atmos. 112, D19304.
Huang, D.S., Zhang, S.Q., 2013. Health benefit evaluation for PM2.5 pollution control in Beijing-Tianjin-Hebei region of China. China Environ. Sci. 33 (1), 166–174.
Hueglin, C., Gehrig, R., Baltensperger, U., Gysel, M., Monn, C., Vonmont, H., 2005. Chemical characterisation of PM2.5, PM10 and coarse particles at urban, near-city and rural sites in Switzerland. Atmos. Environ. 39 (4), 637–651.
Jimenez, J.L., Canagaratna, M.R., Donahue, N.M., Prevot, A.S.H., Zhang, Q., Kroll, J.H., Decarlo, P.F., Allan, J.D., Coe, H., Ng, N.L., Aiken, A.C., Docherty, K.S., Ulbrich, I.M., Grieshop, A.P., Robinson, A.L., Duplissy, J., Smith, J.D., Wilson, K.R., Lanz, V.A., Hueglin, C., Sun, Y., et al., 2009. Evolution of organic aerosols in the atmosphere. Science 326 (5959), 1525–1529.
Kan, H., Chen, B., 2004. Particulate air pollution in urban areas of Shanghai, China: health-based economic assessment. Sci. Total Environ. 322 (1), 71–79.
Lee, E., Chan, C.K., Paatero, P., 1999. Application of positive matrix factorization in source apportionment of particulate pollutants in Hong Kong. Atmos. Environ. 33 (19), 3201–3212.
Lee, P.K.H., Brook, J.R., Dabekzlotorzynska, E., Mabury, S., 2003. Identification of the major sources contributing to PM2.5 observed in Toronto. Environ. Sci. Technol. 37 (21), 4831–4840.
Li, C., Hu, Y., Chen, J., Ma, Z., Ye, X., Yang, X., Wang, L., Wang, X., Mellouki, A., 2016. Physiochemical properties of carbonaceous aerosol from agricultural residue burning: density, volatility, and hygroscopicity. Atmos. Environ. 140, 94–105.
Li, C., Hu, Y., Zhang, F., Chen, J., Ma, Z., Ye, X., Yang, X., Wang, L., Tang, X., Zhang, R., Mu, M., Wang, G., Kan, H., Wang, X., Mellouki, A., 2017. Multi-pollutant emissions from the burning of major agricultural residues in China and the related health-economic effects. Atmos. Chem. Phys. 17, 4957–4988.
Li, P., Xin, J., Wang, Y., Wang, S., Li, G., Pan, X., Liu, Z., Wang, L., 2013. The acute effects of fine particles on respiratory mortality and morbidity in Beijing, 2004–2009. Environ. Sci. Pollut. Res. 20 (9), 6433–6444.
Li, T., Wang, Y., Li, W., Chen, J., Wang, T., Wang, W., 2015. Concentrations and solubility of trace elements in fine particles at a mountain site, southern China: regional sources and cloud processing. Atmos. Chem. Phys. 15 (15), 8987–9002.
Lippmann, M., 2014. Toxicological and epidemiological studies on effects of airborne fibers: coherence and pubic health implications. Crit. Rev. Toxicol. 44 (4), 299–347.
Liu, X., Xie, P., Liu, Z., Tiantian, Li, Zhong, L., 2010. Economic assessment of acute health impact due to inhalable particulate air pollution in the pearl river delta. Acta Sci. Nat. Univ. Pekin. 46 (5), 829–834 (in Chinese).
Mahowald, N.M., 2011. Aerosol indirect effect on biogeochemical cycles and climate. Science 334 (6057), 794–796.
Miri, M., Aval, H.E., Ehrampoush, M.H., Mohammadi, A., Toolabi, A., Nikonahad, A., Derakhshan, Z., Abdollahnejad, A., 2017. Human health impact assessment of exposure to particulate matter: an AirQ software modeling. Environ. Sci. Pollut. Res. 24 (19), 16513–16519.
Miri, M.R., Alahabadi, A., Ehrampoush, M.H., Ghaffari, H.R., Sakhvidi, M.J.Z., Eskandari, M., Rad, A., Lotfi, M.H., Sheikhha, M.H., 2018. Environmental determinants of polycyclic aromatic hydrocarbons exposure at home, at kindergartens and during a commute. Environ. Int. 118, 266–273.
Miri, M.R., Derakhshan, Z., Allahabadi, A., Ahmadi, E., Conti, G.O., Ferrante, M., Aval, H.E., 2016. Mortality and morbidity due to exposure to outdoor air pollution in Mashhad metropolis, Iran. The AirQ model approach. Environ. Res. 151, 451–457.
Polissar, A.V., Hopke, P.K., Harris, J.M., 2001. Source regions for atmospheric aerosol measured at Barrow, Alaska. Environ. Sci. Technol. 35 (21), 4214–4226.
Prendes, P., Andrade, J.M., Lopezmahia, P., Prada, D., 1999. Source apportionment of inorganic ions in airborne urban particles from Coruña city (N.W. of Spain) using positive matrix factorization. Talanta 49 (1), 165–178.
Shi, Y., Chen, J., Hu, D., Wang, L., Yang, X., Wang, X., 2014. Airborne submicron particulate (PM1) pollution in Shanghai, China: chemical variability, formation/dissociation of associated semi-volatile components and the impacts on visibility. Sci. Total Environ. 473, 199–206.
Song, Y., Zhang, Y., Xie, S., Zeng, L., Zheng, M., Salmon, L.G., Shao, M., Slanina, S., 2006. Source apportionment of PM2.5 in Beijing by positive matrix factorization. Atmos. Environ. 40 (8), 1526–1537.
Speer, R.E., Barnes, H.M., Brown, R., 1997. An instrument for measuring the liquid water content of aerosols. Aerosol Sci. Technol. 27 (1), 50–61.
Tao, J., Gao, J., Zhang, L., Zhang, R., Che, H., Zhang, Z., Lin, Z., Jing, J., Cao, J.J., Hsu, S., 2014. PM2.5 pollution in a megacity of southwest China: source apportionment and implication. Atmos. Chem. Phys. 14 (4), 8679–8699.
Tao, J., Shen, Z., Zhu, C., Yue, J., Cao, J., Liu, S., Zhu, L., Zhang, R., 2012. Seasonal variations and chemical characteristics of sub-micrometer particles (PM 1) in Guangzhou, China. Atmos. Res. 118 (3), 222–231.
Turpin, B.J., Huntzicker, J.J., 1995. Identification of secondary organic aerosol episodes and quantitation of primary and secondary organic aerosol concentrations during SCAQS. Atmos. Environ. 29 (23), 3527–3544.
Van Winkle, L.S., Bein, K.J., Anderson, D.S., Pinkerton, K.E., Tablin, F., Wilson, D.W., Wexler, A.S., 2015. Biological dose response to PM2.5: effect of particle extraction method on platelet and lung responses. Toxicol. Sci. 143 (2), 349–359.
Wang, H., Zhuang, Y., Sun, Y., Yuan, H., Zhuang, G., Hao, Z., 2008. Long-term monitoring and source apportionment of PM2.5/PM10 in Beijing, China. J. Environ. Sci. 20 (11), 1323–1327.
Wang, H., Zhuang, Y., Wang, Y., Sun, Y., Yuan, H., Zhuang, G., Hao, Z., 2008. Long-term monitoring and source apportionment of PM2.5/PM10 in Beijing, China. J. Environ. Sci. 20 (11), 1323–1327.
Wang, X., He, S., Chen, S., Zhang, Y., Wang, A., Luo, J., Ye, X., Mo, Z., Wu, L., Xu, P., Cai, G., Chen, Z., Lou, X., 2018. Spatiotemporal characteristics and health risk assessment of heavy metals in PM2.5 in Zhejiang Province. Int. J. Environ. Res. Public Health 15 (4), 583.
Wang, Y., Zhang, X.Y., Arimoto, R., Cao, J.J., Shen, Z., 2004. The transport pathways and sources of PM10 pollution in Beijing during spring 2001, 2002 and 2003. Geophys. Res. Lett. 31 (14), L14110.
Wang, Y., Zhang, X.Y., Draxler, R.R., 2009. TrajStat: GIS-based software that uses various trajectory statistical analysis methods to identify potential sources from long-term air pollution measurement data. Environ. Model. Softw. 24 (8), 938–939.
Watson, J.G., Chow, J.C., Houck, J.E., 2001. PM2.5 chemical source profiles for vehicle exhaust, vegetative burning, geological material, and coal burning in Northwestern Colorado during 1995. Chemosphere 43 (8), 1141–1151.
Weichenthal, S., Villeneuve, P.J., Burnett, R.T., Van Donkelaar, A., Martin, R.V., Jones, R.R., Dellavalle, C.T., Sandler, D.P., Ward, M.H., Hoppin, J., 2014. Long-term exposure to fine particulate matter: association with nonaccidental and cardiovascular mortality in the agricultural health study cohort. Environ. Health Perspect. 122 (6), 609–615.
Xie, P., Liu, X.Y., Liu, Z.R., Li, T.T., Bai, Y.H., 2009. Exposure-response functions for health effects of ambient participate matter pollution applicable for China. China Environ. Sci. 29 (10), 1034–1040.
Xie, Y.B., Chen, J., Li, W., 2014. An assessment of PM2.5 related health risks and impaired values of Beijing residents in a consecutive high-level exposure during heavy haze days. Environ. Sci. 35 (1), 1–8 (in Chinese).
Xu, L., Shu, X., Hollert, H., 2016. Aggregate risk assessment of polycyclic aromatic hydrocarbons from dust in an urban human settlement environment. J. Clean. Prod. 133, 378–388.
Xu, X., Chen, J., Zhu, C., Li, J., Sui, X., Liu, L., Sun, J., 2018;al.,. Fog composition along the Yangtze River basin: detecting emission sources of pollutants in fog water. J. Environ. Sci. 71, 2–12.
Yao, L., Yang, L., Yuan, Q., Yan, C., Dong, C., Meng, C., Sui, X., Yang, F., Lu, Y., Wang, W., 2016. Sources apportionment of PM2.5 in a background site in the North China Plain. Sci. Total Environ. 541, 590–598.
Yao, Q., Li, S., Xu, H.W., Zhuo, J., Song, Q., 2009. Studies on formation and control of combustion particulate matter in China: a review. Energy 34 (9), 1296–1309.
Yassaa, N., Meklati, B.Y., Cecinato, A., Marino, F., 2001. Organic aerosols in urban and waste landfill of Algiers metropolitan area: occurrence and sources. Environ. Sci. Technol. 35 (2), 306–311.
Ye, Z., Li, Q., Ma, S., Zhou, Q., Gu, Y., Su, Y., Chen, Y., Chen, H., Wang, J., Ge, X., 2017. Summertime day-night differences of PM2.5 components (Inorganic Ions, OC, EC, WSOC, WSON, HULIS, and PAHs) in Changzhou, China. Atmosphere 8 (10), 189.
Yin, H., Pizzol, M., Xu, L., 2017. External costs of $PM_{2.5}$ pollution in Beijing, China: uncertainty analysis of multiple health impacts and costs. Environ. Pollut. 226,

356–369.
Yin, H., Xu, L., Cai, Y., 2015. Monetary valuation of PM10-related health risks in Beijing China: the necessity for PM10 pollution indemnity. Int. J. Environ. Res. Public Health 12 (8), 9967–9987.
Ying, I.T., Kuo, S., 2005. PM2.5 aerosol water content and chemical composition in a metropolitan and a coastal area in southern Taiwan. Atmos. Environ. 39 (27), 4827–4839.
Yu, L., Wang, G., Zhang, R., Zhang, L., Song, Y., Wu, B., Li, X., An, K., Chu, J., 2013. Characterization and source apportionment of PM2.5 in an urban environment in Beijing. Aerosol Air Qual. Res. 13 (2), 574–583.
Zhang, M., Song, Y., Cai, X., 2007. A health-based assessment of particulate air pollution in urban areas of Beijing in 2000–2004. Sci. Total Environ. 376 (1–3), 100–108.
Zhang, R., Jing, J., Tao, J., Hsu, S., Wang, G., Cao, J.J., Lee, C.S., Zhu, L., Chen, Z., Zhao, Y., Shen, Z., 2013. Chemical characterization and source apportionment of PM2.5 in Beijing: seasonal perspective. Atmos. Chem. Phys. 13 (14), 7053–7074.
Zheng, M., Salmon, L.G., Schauer, J.J., Zeng, L., Kiang, C.S., Zhang, Y., Cass, G.R., 2005. Seasonal trends in PM2.5 source contributions in Beijing, China. Atmos. Environ. 39 (22), 3967–3976.
Zhou, L., Hopke, P.K., Paatero, P., Ondov, J.M., Pancras, J.P., Pekney, N.J., Davidson, C.I., 2004. Advanced factor analysis for multiple time resolution aerosol composition data. Atmos. Environ. 38 (29), 4909–4920.
Zong, Z., Wang, X., Tian, C., Chen, Y., Qu, L., Ji, L., Zhi, G., Li, J., Zhang, G., 2016. Source apportionment of PM2.5 at a regional background site in North China using PMF linked with radiocarbon analysis: insight into the contribution of biomass burning. Atmos. Chem. Phys. 16, 11249–11265.